Superconducting and transport properties of (Bi–Pb)–Sr–Ca–Cu–O with Cr_2O_3 additions

H. Abbasi*, J. Taghipour, H. Sedghi

Department of Physics, Superconductivity Research Center, University of Urmia, Urmia, Iran

ARTICLE INFO

ABSTRACT

The effect of Cr_2O_3 additions in (Bi, Pb)–Sr–Ca–Cu–O superconductors using the conventional solid-state reaction method is reported. Cr_2O_3 with 0, 0.3, 0.5, 0.7, and 1.0 wt.% were added to the (Bi, Pb)–Sr–Ca–Cu–O system. The critical temperature (T_C) and transport critical current density (J_C) were determined by the four-point probe technique. The phases in the samples were determined using the powder X-ray diffraction method. The maximum T_C and J_C were observed for the sample with 0.5 wt.% Cr_2O_3. The variation in the J_C of all the samples was explained by the effective flux pinning by Cr_2O_3 in the samples.

1. Introduction

Following the discovery of the Bi–Sr–Ca–Cu–O superconductor system [1,2], worldwide research efforts to improve its superconducting properties have been actively undertaken [3–6]. To enhance its current-carrying capacity, various methods have been employed, including introducing artificial flux pinning. The critical temperature, T_C, and critical current density, J_C, are found to increase with Gd substitution at the Sr site [7]. At 77 K, the self-field J_C of the samples with added Nd was found to be much higher than the undoped one [8]. In particular a small amount of chromium oxide doping improves the flux pinning, with the effective pinning center due to Cr substitution for Cu, while excessive Cr-ion doping degrades the superconductivity of $Bi_{1.66}Pb_{.34}Sr_2Ca_2Cu_3O_{10}$ (2223) [9]. The T_C of Cr-doped Bi–Sr–Ca–Cu–O decreased due to the decrease of the hole concentration through substitution of Cr^{3+} for Cu^{2+}. The substitution also causes appreciable change in the normal-state conductivity [10]. Proper Cr doping seems to be a convenient and effective method to introduce artificial defects into the Bi2223 system as pinning centers [11]. To the best of our knowledge, Cr_2O_3 additions in Bi–Sr–Ca–Cu–O superconductors have not yet been reported. Hence, it is interesting to investigate the effect of Cr_2O_3 in the Bi–Sr–Ca–Cu–O system. In this paper, we report the effect of Cr_2O_3 additions in Bi–Sr–Ca–Cu–O particularly with respect to T_C and J_C.

2. Experimental

The $Bi_{1.66}Pb_{.34}Sr_2Ca_2Cu_3O_{10}$ samples were prepared from ultra-fine powders Bi_2O_3 (99.99%), PbO (99.99%), CuO (99.99%), $SrCO_3$ (99.99%) and $CaCO_3$ (99.99%) using the conventional solid-state reaction method [12]. The starting powders were weighed and well mixed in stoichiometric proportions calcined at 810 °C in air for 24 h to remove any remaining volatile materials and to start the formation of the superconducting phases. The resulting powder from the calcinations process pressed in to pellets, and sintered at 850 °C in air for 140 h with several intermediate grinding processes. Cr_2O_3 with amounts of 0.3, 0.5, 0.7, and 1.0 wt.% were added to the $Bi_{1.66}Pb_{.34}Sr_2Ca_2Cu_3O_{10}$ powder and well mixed. Samples were pressed into pellets with 13 mm diameter and 2 mm thickness and sintered at 860 °C for 48 h. The electrical resistance-temperature measurements were carried out by the four-probe technique using OXFORD-ITC502 closed cycle refrigerator and a Lock-in Amplifier at temperatures between 40 and 300 K. The magnetic field was applied parallel to the current direction. The external DC magnetic fields for resistivity measurements were provided by an electromagnet. The critical current density was measured on bar-shape samples between 30 and 77 K using the 1 μV/cm criterion. Powder X-ray diffraction patterns were recorded using a PHILIPS XPERT X-ray diffractometer. Energy dispersive X-ray (EDX) analyses were performed by OXFORD EDX (coupled to a SEM Model LEO-1450VP).

The relative volume fractions of the Bi2223 and Bi2212 phases in all samples were calculated using the following set of equations [13,14]:

$$\text{Bi2223 (\%)} \approx \frac{\sum I(\text{Bi2223})}{\sum I(\text{Bi2223}) + \sum I(\text{Bi2212})} \times 100 \tag{1}$$

$$\text{Bi2212 (\%)} \approx \frac{\sum I(\text{Bi2212})}{\sum I(\text{Bi2223}) + \sum I(\text{Bi2212})} \times 100 \tag{2}$$

where I is the intensity of the Bi2223 and Bi2212 phases (Fig. 1).

* Corresponding author. Tel.: +98 09144818347; fax: +98 04812243311.
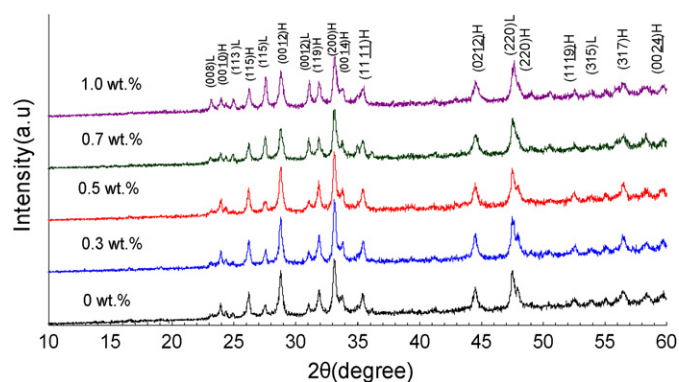 E-mail address: st_h.abbasi@urmia.ac.ir (H. Abbasi).

Fig. 1. X-ray diffraction pattern of samples.

3. Results and discussion

Fig. 1 shows the XRD patterns of the samples. The samples consist of 2223 as the major phase and 2212 as the minor phase. H and L indicate the high-T_C 2223 phase and low-T_C 2212 phase, respectively. In addition, the XRD results show that Cu was partially substituted by Cr (XRD results show $Bi_{1.66}Pb_{.34}Sr_2Ca_2Cu_{3-x}Cr_xO_y$ formula for samples). The substitution of Cr at Cu-site was confirmed by the energy dispersive X-ray analyses. The addition of Sb into Bi2223 system was observed. The percentage of the 2223 and 2212 phases calculated using Eqs. (1) and (2), are given in Table 1 [13,14]. The volume fraction of the 2223 phase for the sample with 0.5 wt.% Cr_2O_3 shows the highest percentage (82.25%). And with further increasing Cr_2O_3 the percentage of the 2223 phase decreases and the percentage of 2212 phase increases. The lattice parameters were determined from ($h\,0\,0$) and ($0\,0\,l$) peaks of the XRD data and they are given in Table 1. The length of the a- and c-axis decrease upon increasing Cr_2O_3 dopant from sample 0 wt.% to sample 1.0 wt.%. The behavior of the lattice parameter can be explained by the decrease of the oxygen content in the unit cell by the replacement of Cr-ion by Cu-ion in the structure. ×, the grain boundaries are in more over-doped regime. These over-doped regions reduce the intergranular coupling and increase weak-link behavior of Cr_2O_3 doped samples. We know that as a result of increase in the weak links between superconducting grains, superconducting samples show lower critical temperature.

Fig. 2 shows the curve of electrical resistance versus temperature for the samples. The $T_{C\text{-zero}}$ for the 0.5 wt.% Cr_2O_3 is the highest (108.56 K) and lowest normal-state resistivity (2.01 (mΩ cm)), whereas the undoped sample exhibited a $T_{C\text{-zero}}$ of 105.42 K and normal-state resistivity of 2.37 mΩ cm. It is believed that the decrease in normal-state resistivity is related to the structural phase transformation (from 2212 to 2223) and weak-links improvement between the grains in the samples. The possible resistance decrease between grains in Cr_2O_3 undoped and doped samples owe to accumulation of Cr at grain boundaries. The presence of significant concentration of Cr atoms at the grain boundary regions would naturally transform the superconductor–insulator–superconductor (SIS) type configura-
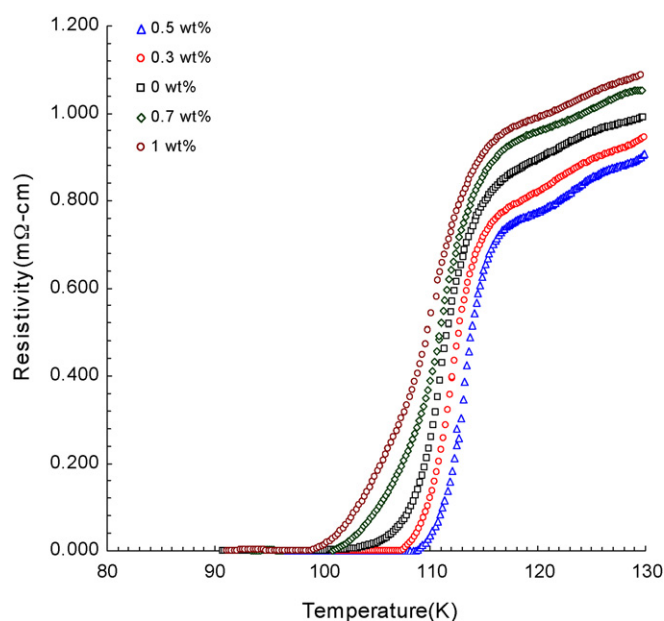

Fig. 2. Resistivity as a function of temperature for samples.

tion into superconductor–normal metal–superconductor (SNS) type. The minimum value of the room temperature resistivity of sample 0.5 wt.% Cr_2O_3 exhibits that it has greater connectivity between the grain boundaries as compared to the other samples (SIS → SNS). The behavior of intergrain boundaries is supported by EDX measurements.

The anomalous $T_{C\text{-zero}}$ for the $x = 0.5$ wt.% sample may be due to homogeneity in the sample and effective pinning centers due to Cr substitution for Cu, while excessive Cr-ion doping degraded the superconductivity of Bi2223, which can affect the transport properties in this type of materials [15,16]. The lower zero resistance transition temperature with increasing Cr_2O_3 content could be interpreted as a result of the suppression of superconductivity by the Cr^{3+} ions. It was observed that Cr_2O_3 doped samples showed a broader transition, which indicates presence of impurities and weak links between superconducting grains. Broadening of the transition width indicates that the Cr_2O_3 doped samples have lower percentage of the Bi2223 phase compared to sample 0 wt.% Cr_2O_3. The structural phase transformation is supported by XRD measurements.

Magnetoresistivity measurements were done under different DC magnetic fields (0, 0.3 and 0.6 T). Under applied magnetic field, the weak links are affected and therefore, the tail part dissipates in even small fields. In large magnetic fields, due to flux penetration inside the grains the onset part of transition will be broadened.

Fig. 3 shows the magnetoresistivity measurements of the samples 0, 0.5 and 1.0 wt.%. As can be seen from Fig. 3 when applied magnetic field increases, the normal-state resistivity of samples does not change considerably, but the resistivity transition width increases with increasing applied magnetic field. The amount of the

Table 1

The results of XRD, lattice parameter c, and resistivity measurements of samples.

x wt.% Cr_2O_3	Bi2223 (%)	Bi2212 (%)	T_C ($R=0$)	ρ ($T=294$ K) (mΩ cm)	Unit cell (Bi2223 phase)	
					a (Å)	c (Å)
0	71.25	28.71	105.42	2.37	5.41	37.30
0.3	73.37	25.14	108.99	2.18	5.40	37.28
0.5	82.25	18.63	108.56	2.01	5.40	37.25
0.7	68.45	31.28	102.57	2.54	5.37	37.22
1.0	63.36	35.96	101.20	2.69	5.35	37.18